A CHANNEL SOUNDER FOR LOW FREQUENCY SUB-SURFACE RADIO PATHS

D. Gibson and M. Darnell

Institute of Integrated Information Systems, University of Leeds, Leeds, LS2 9JT, UK
D.Gibson@caves.org.uk M.Darnell@elec-eng.leeds.ac.uk

ABSTRACT: In an application to measure subterranean radio propagation, a wide-band low-frequency channel sounder makes use of a modified pseudo-random binary sequence, which is cross-correlated with its inverse at the receiver, and which uses a code-locked loop to maintain synchronism with the transmitter. The transmitting antenna for such a system is essentially an induction loop, and the extreme wideband nature of the system requires this to be operated untuned. The resultant low efficiency is countered by using a suitable binary sequence at the transmitter and signal-averaging techniques at the receiver.

1 INTRODUCTION: SUB-SURFACE RADIO

This paper describes an application of DSP techniques to sub-surface digital radio communications. In particular it describes a system for performing channel-sounding experiments in the VLF, voice and LF bands (300Hz to 300kHz). A discussion of sub-surface radio systems, with reference to the peculiarities of the propagation, antenna requirements and the development of an adaptive digital communications system has already been given [1]. To recap., the features that characterise these systems are

i) Communications through conductive media over distances of only a few skin depths – but not restricted to near field.

ii) Small, portable antennas. (Large fixed installations are used by the mining industry).

iii) Restricted choice of frequency. (Interference, noise, other primary channel users).

iv) Optimum frequency and orientation of antenna depends on many external factors, including transmission distance and ground conductivity, as well as noise and co-channel interference.

Induction radio has been used for communications in the mining industry, and also by cavers and pot-holers. In addition to speech communications, radiolocation and cave surveying beacons make use of the known behaviour of the near-field lines, so accurate results are limited to under a skin depth, although deeper work is possible when a more accurate propagation model is used [2]. Archaeological and geophysical applications include the remote measurement of ground conductivity by analysing the phase of the induced fields from an induction loop.

Subterranean radio systems differ from the ELF (30–300Hz) systems, which have been developed for submarine communications, because the latter operate in the far field – at 300Hz the transition distance is at 160km in air, and only 15m in sea-water. The analysis of such systems involves concepts that are not applicable to a subterranean radio system. Cave radios differ from mine communications systems because they usually use small, portable antennas and a low power, whereas a mining application can use a large, powerful, fixed antenna, and needs to address the problem of transmission through conductive over-burden to deep workings.

2 CHANNEL SOUNDING

2.1 Uses of channel sounding

Propagation in a conductive medium, although well studied, can still be difficult to describe succinctly. Channel sounding, as well as providing the practical means to determine the optimum operation of a communication system, will allow us to test the theory and to develop some simple and instructive models of the propagation. In addition, the same equipment can be used to make measurements of background noise and interference at a high resolution, in a similar manner to that reported by Laflin [3]. Because channel sounding is a swift, automated exercise we will be able to make measurements at many locations underground, under a range of different conditions. It is planned to use specially-designed datalogging equipment to capture data at remote locations over a period of many months.

2.2 Measurement Spectrum

Almost the entire LF band (30-300kHz) has been used for subsurface communications at one time or another, but most through-rock communications takes place at 80-100kHz in the UK and Europe. In

areas with much drier rock, 185kHz is a popular choice of frequency. Beacon communications (e.g. for radiolocation or telemetry) tend to be in the voice frequency band at 0.3-3kHz. We might, eventually, wish to evaluate the spectrum over three decades, from 300Hz to 300kHz, although an initial investigation of propagation, noise and interference will be restricted to the band from 15kHz to 240kHz (a range of 16:1). This range encompasses several existing amateur and commercial designs of beacon and radio [4].

2.3 Experimental Method

The sounding signal is a wideband binary sequence. The original intention was to use a high-speed data-capture board and a laptop PC to test the system in the field. However, problems arose because of the power consumption and the large amount of real-time data – 32Mbytes per sounding – that needs to be captured. Instead, some dedicated hardware is being developed around an industrial datalogger. The data is reduced in real time to 512kbytes/dataset. Multiple datasets are stored on a 500Mb hard disc contained in a PCMCIA card. A block diagram showing the salient features of the channel sounder is shown in ***Figure 1***. The features can be summarised as

- 256 bit sequence (modified PRB sequence) clocked at 256kHz (1kHz spectral lines)
- Data capture: 65536 samples in 256ms (spectrum information at 3.9Hz intervals)
- Signal averaging of 256 sample sets in 66s (total 16M samples, increases SNR by 24dB)
- 65536-point FFT to obtain spectrum

For sounding purposes we do not need a particularly fine resolution so, initially, we are using a 256-chip sequence, clocked at around 256kHz. The spectral lines will therefore be 1kHz apart. The equipment is capable of generating much longer sequences than this. A 256-point FFT would be sufficient to extract meaningful data, but sampling in greater detail allows us to view the background noise and interfering signals at a high resolution, in a similar manner to that reported by Laflin [3]. We will collect 2^{16} samples, taking 256ms to do so, and resulting in spectrum information every 3.9Hz. We will use signal averaging to increase the SNR, collecting 2^8 sample sets of 2^{16} samples in 66s. This increases the SNR by 24dB, and reduces the noise-equivalent bandwidth by 256 times from something of the order of 3.9Hz (depending on the FFT details) to 0.015Hz. This requires the receiver to maintain a very good synchronism to the transmitter, which is achieved using a code-locked loop (***Figure 2***) which, in turn, requires attention to the sequence design to ensure that a good impulse response can be extracted at the receiver.

3 EQUIPMENT DESIGN

3.1 Transmitter Antenna

Without a careful analysis, it is not always clear whether, for inductive communications with portable equipment, an air-cored loop makes a better transmitter antenna than a ferrite-cored solenoid. But whichever type of antenna is used it will, unless physically very large, present a mainly inductive load to the driver. The power transfer efficiency of an analogue power amplifier drops by a factor of $Q = j\omega L/R$ when the load is inductive. We could envisage a spot-frequency system with some method of re-tuning the antenna between measurements, but this would probably require a cumbersome and time-consuming mechanical tuning system.

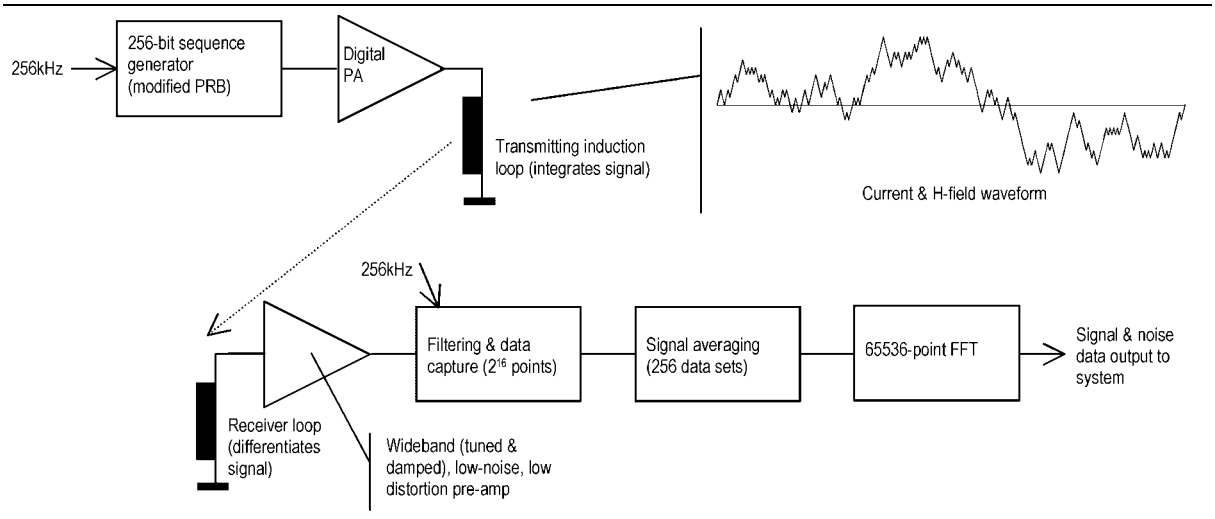

Figure 1 – Block diagram of prototype channel-sounding system

It seems clear that using an untuned wideband transmitter is the correct approach for our extremely wideband signal – a 16:1 frequency range, initially). It is desirable to drive such an antenna from a digital complementary output stage so that the issue of PA efficiency does not arise. However, it is still the case that, for a given driving voltage, the magnetic moment is lower, by a factor of *Q*, than it would be for a purely resistive loop. We have the choice of several methods of excitation – e.g. spot frequency, chirp, pseudo-random sequence and, of these, the wideband PRB sequence seems the most attractive.

As noted above, the magnetic moment is reduced by a factor of *Q* for single frequencies. However, driving the loop with a wideband NRZ signal allows us to utilise more power, owing to the presence of low frequency components in the signal. We have deduced, from a circuit simulation, that a 256 chip near-random sequence will allow us to drive the antenna with 256 times more power than if we used a simple 010101… sequence at the same chip rate. Even so, the amount of power we can send to the antenna is limited.

This sequence is integrated by the transmitter antenna to give a current waveform as shown in ***Figure 1*** above, and is differentiated at the receiver antenna. The power spectrum for the integrated PRB sequence drops off smoothly at 6dB/octave for frequencies below the chip-rate. Since atmospheric noise also drops with frequency, this may turn out to be an appropriate spectrum to use.

3.2 Choice of Sequence

Using a maximal-length pseudo-random binary (PRB) sequence poses a problem, because binary *m*-sequences are of period 2^n-1 and thus cannot be used directly with the most efficient form of FFT, which requires a sequence of period 2^n. Two well-known solutions [5] to this problem are i) to ignore it, and to pretend that the continuous signal has a period of 2^n; and ii) to use the inverse Fourier transform to generate the test data itself. In the latter case, the resulting test signal will have the prescribed length and power spectrum, but will, unfortunately, consist of non-binary values whereas, for PA efficiency, we need a binary sequence, so that we can use a digital or class-D power amplifer.

The solution we have adopted is to take a maximal-length PRB sequence and add one bit, to make a sequence of length 2^n. The position of the added bit affects the size of the sidelobes in the auto-correlation function (ACF) but, by trial and error, it is possible to find the sequence with the lowest sidelobes. Clearly, the precise power spectrum of the sequence does not matter for simple spectral measurements of attenuation and phase shift – the situation regarding impulse response will be discussed below). This '*M*+1' sequence gives us the added advantage that, because it has no d.c. content, the induction loop (which acts as an integrator) will not cause the current to ramp over time. The sequence is shown in ***Table 1***, below. Its ACF is shown in ***Figure 3***. (This and other graphs appear at the end of this paper).

```
10110001,11101000,01111111,10010000,
10010011,11101010,10111000,00110001,
01011001,10010111,11101111,00110111,
01110010,10100101,00010010,11010001,
10011100,11110001,10110000,10001011,
10101111,01101111,10000110,10011010,
11011010,10000010,01110110,01001001,
10000001,11010010,00111000,10000000.
```

Table 1 –Unipolar M+1 sequence

The chosen sequence was obtained by adding one bit (shown bold and underlined) to a 255-bit binary M-sequence.

3.3 Cross-correlation with inverse sequence

Although the choice of sequence is not crucial for spectral measurements, a sequence with a good auto-correlation (i.e. minimal sidelobes) is necessary for measurements of the channel's impulse response. A good ACF is also required for operation of the receiver's code-locked loop (CLL), which will be explained later. In general terms, we can transmit a time sequence $F(t)$ of period T and correlate this with a sequence in the receiver, such that we obtain the ideal CCF, a delta function. We can therefore ***define*** the receiver's copy of the sequence as the ***inverse***, $F^{-1}(t)$ of the transmitted sequence, and note that we desire

$$R(\tau) = \frac{1}{T}\int_0^T F(t)\cdot F^{-1}(t+\tau)\cdot dt \quad = \delta(\tau) \qquad (1)$$

Where $\delta(t)$=1 if t=0, and zero otherwise. If $F(t)$ were, for example, a unipolar binary *M*-sequence (1,0,0,1...) then we could note that its inverse would be a suitably scaled bipolar version of the same sequence (1,-1,-1,1...).

It is possible [6, 7] to define an inverse sequence that satisfies the above property for any periodic function, provided that its discrete Fourier transform contains no zeroes in the frequency domain. We can derive

$$F^{-1}(t) = F(t) \oplus \boldsymbol{f}^{-1}\left(\frac{T}{\boldsymbol{f}(F(t))}\right)^2 \qquad (2)$$

where $\boldsymbol{f}$ denotes the discrete Fourier transform, defined such that $\boldsymbol{f}(1) = T\,\delta$; T denotes the length of the sequence, and $\oplus$ denotes the cross-correlation defined in (1), with

$$F \oplus F^{-1} = \delta \qquad (3)$$

Equation (2) is a useful result because of the imperfect ACF of our chosen M+1 sequence. Cross-correlating the unipolar sequence of ***Table 1*** with its inverse sequence listed in ***Table 2*** (below) results in a delta function of unity amplitude. The sequence in ***Table 2*** was calculated to three significant figures; the CCF is plotted in ***Figure 4*** and shows an r.m.s. sidelobe level below -74dB. With five-figure accuracy this increases to -112dB. We observe that the inverse is multi-valued. This is to be expected, of course, but this it poses no problems because it is the *transmitted* sequence that must be binary, for reasons of transmitter efficiency. ***Table 2*** is plotted in ***Figure 7*** at the end of this document.

```
-0.59, -0.64,  2.18,  1.55, -2.61, -2.11, -1.00,  0.04,
 3.62,  0.53,  2.58, -2.03,  2.69, -1.79, -1.83, -1.13,
-3.08,  1.01,  1.40,  2.82,  1.05,  1.88,  2.90,  1.57,
 3.13, -0.96, -2.25,  1.79, -2.31, -1.31, -2.10, -2.75,
 1.69, -2.02,  0.42,  2.05, -4.10,  0.39,  2.21,  2.47,
 1.91,  1.47,  1.71, -3.07,  2.53, -2.25,  0.76, -0.61,
 0.89, -0.80,  1.65,  3.48, -0.13, -1.82, -1.49, -4.20,
-1.75, -0.17,  1.57,  4.11, -5.48, -1.04, -3.00,  4.39,
-3.07,  3.34, -3.43,  3.93,  0.70, -1.70, -1.63,  1.67,
 3.06, -5.11,  0.00,  1.59, -0.57,  1.49,  2.52,  1.50,
 2.39,  1.75,  3.45, -4.81,  3.86,  1.23,  2.77,  0.87,
-2.65, -1.46,  3.06,  1.46, -1.92,  2.35,  2.18,  2.43,
-2.29,  1.42,  2.10,  1.09, -3.08,  0.28,  0.22, -1.43,
 1.05, -1.13,  3.54, -4.84, -0.31,  1.17, -2.62,  3.65,
-2.97, -3.08, -0.71,  2.05, -1.80, -2.91,  2.37, -3.19,
 5.01,  0.85, -1.12, -0.50, -1.53, -1.05, -3.55,  4.00,
 1.04, -1.96, -3.00,  3.36,  1.25,  2.72, -3.82, -1.49,
 2.91,  1.91,  2.06,  1.54, -2.54,  1.49, -5.22,  3.93,
-0.44,  0.35,  1.02,  1.98, -1.14, -2.32, -2.76, -0.24,
 1.21, -1.44, -3.83, -0.94,  2.13, -1.94,  2.25,  1.00,
 3.04, -2.09,  1.95, -1.59,  0.32,  3.00,  1.87,  1.77,
-1.24,  0.01,  3.66, -4.73,  5.57, -1.30,  4.17,  2.10,
 2.45, -1.73, -2.22, -4.35,  0.63,  0.44,  3.70, -4.67,
 4.16, -0.59, -4.27,  3.63,  1.01, -0.19,  0.70, -0.53,
-1.57,  4.47, -2.20,  1.96,  1.26, -0.91,  2.42, -3.06,
 1.81, -1.56, -0.99, -4.01, -0.65, -3.38,  2.44,  0.12,
-4.09,  3.10,  0.75,  1.97, -0.53,  0.03,  3.90, -2.81,
-3.61,  3.07, -2.07, -0.56,  0.01,  1.52, -3.62,  1.15,
 1.88, -1.41, -2.18, -1.11, -1.09, -1.56, -3.55,  3.00,
-0.66,  4.12, -0.35, -1.29, -0.86, -2.22,  2.17, -1.82,
-2.17, -0.16, -0.63,  2.22,  2.48, -1.36,  0.53, -7.71,
 5.26, -2.46, -1.25, -3.23, -2.12, -0.75, -1.78, -2.08.
```

Table 2 – Inverse of unipolar M+1 sequence

The sequence in Table 1 is unipolar, so it is possible to calculate an inverse sequence. The CCF of the sequence with its inverse gives a unity impulse. (values in table read across then down)

The sequence in ***Table 1*** is unipolar. However, the received sequence will have no zero-frequency (d.c.) component; it will be bipolar and so its inverse cannot be calculated. This is a trivial situation since we could – in theory at least – restore the d.c. level at the receiver. If the incoming sequence $F'(t)$ were bipolar (values all ±½, defined by $F' = F - ½$) then we could add ½ to it, and perform the correlation (notated by ⊕) to get

$$\left(F'(t) + \underbrace{½}_{\text{dc level restored}} \right) \oplus F^{-1}(t) = \delta(\tau) \qquad (4)$$

but, since correlation is a linear operation, we can rearrange this to show that the output of the correlator without this correction factor, would be

$$F'(t) \oplus F^{-1}(t) = \delta(\tau) - \underbrace{½ \oplus F^{-1}(t)}_{\text{d.c. level superimposed on output}} \qquad (5)$$

This shows that, although $F^{-1}(t)$ is not the true inverse of $F'(t)$, the effect is simply to add a small constant to the output. This conclusion is easily verified by simulation, as follows…

i) The bipolar sequence {½, -½, ½, ½, -½, -½, -½, ½,…} has ½ added, resulting in the unipolar sequence {1,0,1,1,0,0,0,1,…} (***Table 1***). A simple *MatLab* simulation can then correlate this with the inverse {-0.59, -0.64, 2.18…}, which results in a delta function with a correlation peak of 1 unit, as shown in ***Figure 4***.

ii) Without the restored d.c. level, the sequence {½, -½, ½, ½, -½, -½, -½, ½,…} correlates to give a peak of 255/256 units, alongside a nearly constant sidelobe level of –1/255 times the peak; the simulation shown in ***Figure 5***. This equates to a CCF of δ - 1/256.

The sidelobes are due to the rounding errors in $F^{-1}(t)$. With a 'long' floating point format in *MatLab*, it is clear that the constant term in (5) – namely ½ ⊕ $F^{-1}(t)$ – is exactly 1/256; i.e. the sum of the coefficients in ***Table 2*** is exactly 2 – a point which would bear further mathematical investigation. These observations about the d.c. level have been explained at length here, but they are actually fairly trivial, being analogous to the fact that the ACF of a bipolar M sequence is $\delta - 1/M$.

3.4 Code-locked Loop

Because we are dealing with very low signal levels we are using a form of signal averaging which

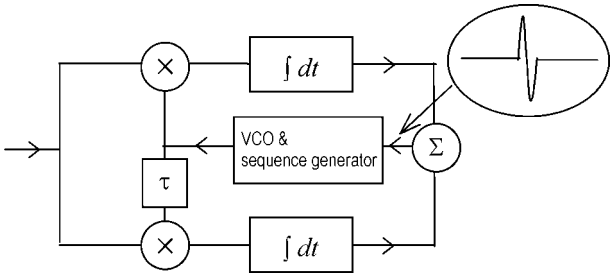

In a standard technique, two correlations are performed – one with an 'early' copy of the inverse sequence and one with a 'late' copy; with a relative time-shift of one 'chip' (τ) *between the two copies. The two CCFs are differenced and the result is a bipolar error signal that is used to control the master clock frequency to bring the system into lock, in a similar way to that of a conventional phase-locked loop.*

Figure 2 – Operation of a code-locked loop.

requires very long sample times, of the order of 30–60s. For the receiver's sample frequency to remain locked to the transmitter over this length of time we require to extract a synchronisation signal from the sounding sequence, by cross-correlating it with its inverse in the receiver. A standard method uses a code-locked (or delay-locked) loop (CLL), as shown in ***Figure 2*** above. This requires two correlations – one with an 'early' copy of the inverse sequence and one with a 'late' copy; with a relative time-shift of one 'chip' between the two copies. The two CCFs are differenced and the result is a bipolar error signal that is used to control the master clock frequency to bring the system into lock, in a similar way to that of a conventional phase-locked loop.

Equation (5) shows that the correlations result in a d.c. level, but we know from the near-ideal CCF in ***Figure 4*** that there is very little ripple in the sidelobes, so the action of taking the difference between the 'early' and 'late' correlations must be to cause the d.c. level to almost cancel, providing us with ideal feedback for the code-locked loop. The CLL feedback signal is shown in ***Figure 6***. Again, this result is a fairly trivial observation and, if the ripple in the sidelobes was large it could not be cancelled by this 'early' – 'late' operation.

3.5 Receiver Antenna

The design of the receiver front-end owes more to low-noise audio design than to r.f. techniques; impedance matching, for example, is not an issue. However, in order to obtain the best SNR, ***noise-matching*** is important. This aspect of the design was outlined in [1].

4 RESULTS

Practical results obtained using the sounder in UK caves will be presented at the symposium.

5 CONCLUDING REMARKS

This paper has briefly described the design of a wideband channel sounder, which can also be used for noise and interference measurements in the LF band. The salient points of the design are as follows.

i. The extreme wideband nature of the sounding signal requires a careful approach to the antenna design and includes the necessity to transmit a binary (two level) sequence.

ii. For ease of processing this must be of length 2^n but such a sequence has a poor auto-correlation property.

iii. The low signal levels imply a long sampling time, and so good synchronisation between the receiver and transmitter is important.

iv. This is achieved by calculating an inverse to the transmitted sequence and cross-correlating the two to obtain the impulse response of the system.

v. The transmitted signal remains bi-valued for efficiency, but the inverse sequence is multi-valued.

vi. The bipolar nature of the received sequence means an exact inverse cannot be calculated, but the error gives rise to a constant term, which does not affect the operation of the code-locked synchronisation loop.

This sounder is part of an adaptive communications system already described [1]. The next phase of the research programme will be to validate our propagation model via practical sounding measurements and to collect data on noise and interference in the LF band. A complete adaptive data transmission system architecture will then be tested.

6 REFERENCES

1 Gibson, D. & M. Darnell (1999), *Adaptive digital communications for sub-surface radio paths*, Proc. DSPCS '99, pp237-244.

2 Gibson, David (2000), *A channel sounder for sub-surface communications: part 2 – Computer simulation of a small buried loop*, CREGJ **41**, pp29-32, Sept 2000

3 Laflin, M.G.(1992), *ELF/VLF spectrum measurements*, AGARD-CP-529, pp17-1 to 17-12. (Conference Proceedings **529** on ELF/VLF/LF Radio Propagation and Systems Aspects; Advisory Group for Aerospace Research and Development; NATO).

4 Gibson, David (1997), *LF utility stations*, BCRA Cave Radio & Electronics Journal **28**, pp16-17, June 97, ISSN 1361-4800.

5 Wellstead, P.E. (1975), *Pseudonoise test signals and the fast Fourier transform*, IEE Electronics Letters, **11**(10), 15 May 1975

6 Al-Dabbagh, A & M. Darnell, A. Noble, S. Farquhar (1997), *Accurate system identification using inputs with imperfect autocorrelation properties*, IEE Electronics Letters **33**(17), pp 1450-1451, 14th August 1997.

7 Al-Dabbagh, A & M. Darnell (1999), *A novel channel estimation technique for radio communications*, DSPCS '99, pp245-251.

Figures 3-7 are printed on the next page...

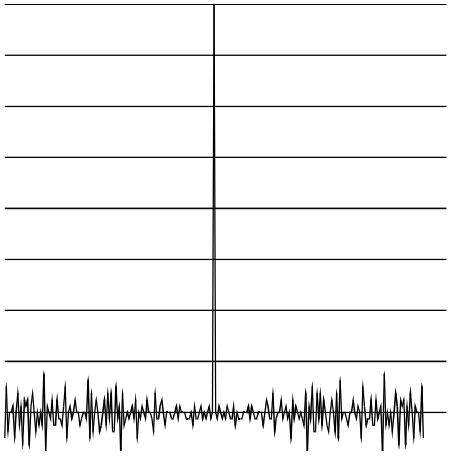

Figure 3 – ACF of M+1 sequence (linear scale)

The ACF of the sequence in Table 1 shows fairly high sidelobes, at up to –21dB. The r.m.s. value of the sidelobe function is –30dB. (The r.m.s. of the peak is -24dB [1/√256] of course, so the peak / sidelobe energy ratio is only 6dB). Y axis is linear, with values 0–1.

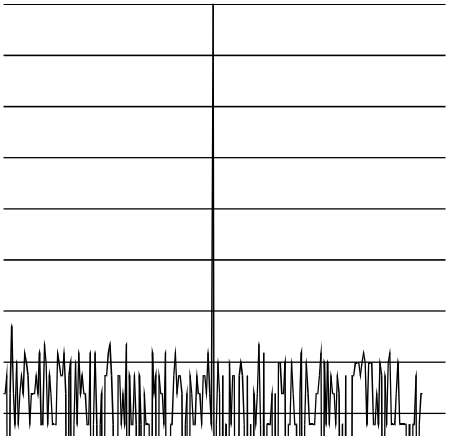

Figure 4 – CCF of unipolar M+1 sequence with its inverse (log scale)

The CCF of the unipolar sequence in Table 1 with its inverse from Table 2 gives a result with sidelobes all below -63dB.
The r.m.s. value of the sidelobe function is –74dB.
With a higher-precision inverse the CCF comes close to an ideal delta-function. Y-axis is 10dB/division.

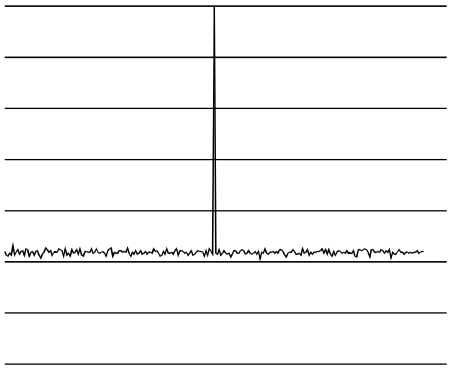

Figure 5 – CCF of bipolar M+1 sequence with the unipolar inverse (log scale)

The near-ideal CCF of Figure 4 has very little sidelobe energy. If, instead, the correlation is performed with a bipolar version of the M+1 sequence, the sidelobes have a near-constant level of 1/255 of the peak.
(r.m.s. of sidelobe function is –48dB).
Y-axis 10dB/division.

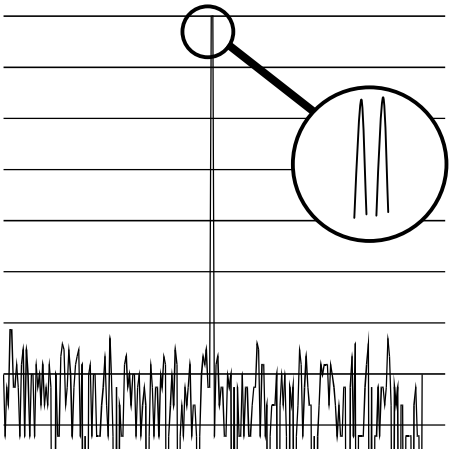

Figure 6 – Sum of Early–Late CCFs

The sum of 'early' minus 'late' CCFs of Figure 4 includes the characteristic double-peak not visible at the scale of this plot.
The bipolar sequence in Figure 5 has a CCF that shows an almost identical early/late result, despite the higher sidelobe level, because the level is largely constant.
Y-axis 10dB/division.

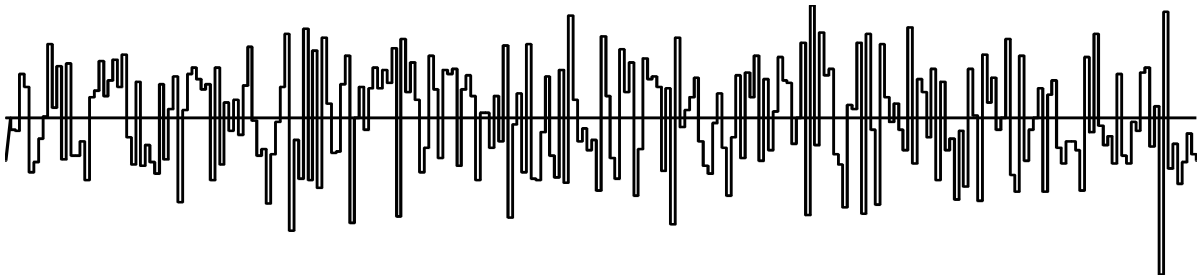

Figure 7 – The Inverse Sequence of Table 2.